

Electronic Supplementary Information (ESI) for

Mg(H₂O)₆[(IO₂(OH))₂(IO₃)₂]: a new iodate with very large ultraviolet cutoff edge and optical anisotropy

Yang Li and Kang Min Ok*

Department of Chemistry, Sogang University, 35 Baekbeom-ro, Mapo-gu, Seoul 04107, Korea

*E-mail: kmok@sogang.ac.kr

Table of contents

Sections	Titles	page
Table S1.	Crystallographic data and structure refinement for Mg(H ₂ O) ₆ [(IO ₂ (OH)) ₂ (IO ₃) ₂].	S2
Table S2.	Atomic coordinates ($\times 10^4$), equivalent isotropic displacement parameters ($\text{\AA}^2 \times 10^3$) and bond valence sum calculations for Mg(H ₂ O) ₆ [(IO ₂ (OH)) ₂ (IO ₃) ₂].	S3
Table S3.	Selected bond lengths (\AA) for Mg(H ₂ O) ₆ [(IO ₂ (OH)) ₂ (IO ₃) ₂].	S4
Table S4.	Selected angles ($^\circ$) for Mg(H ₂ O) ₆ [(IO ₂ (OH)) ₂ (IO ₃) ₂].	S5
Table S5.	Hydrogen atom coordinates ($\text{\AA} \times 10^4$) and isotropic displacement parameters ($\text{\AA}^2 \times 10^3$) for Mg(H ₂ O) ₆ [(IO ₂ (OH)) ₂ (IO ₃) ₂].	S5
Table S6.	Hydrogen bonds in Mg(H ₂ O) ₆ [(IO ₂ (OH)) ₂ (IO ₃) ₂].	S6
Table S7	List of reported birefringence compounds in alkali, alkaline earth, and rare earth metal cations-containing iodates/fluoroiodates system.	S7
Fig. S1.	Asymmetric unit of Mg(H ₂ O) ₆ [(IO ₂ (OH)) ₂ (IO ₃) ₂]. The ellipsoids are drawn at 50% probability level.	S8
Fig. S2.	IR spectrum of Mg(H ₂ O) ₆ [(IO ₂ (OH)) ₂ (IO ₃) ₂].	S9
Fig. S3.	TGA and DSC diagrams of Mg(H ₂ O) ₆ [(IO ₂ (OH)) ₂ (IO ₃) ₂].	S10
Fig. S4.	Band structure for Mg(H ₂ O) ₆ [(IO ₂ (OH)) ₂ (IO ₃) ₂].	S11
Fig. S5.	The electron density difference map of Mg(H ₂ O) ₆ [(IO ₂ (OH)) ₂ (IO ₃) ₂].	S12
References		S13

Table S1. Crystallographic data and structure refinement for Mg(H₂O)₆[(IO₂(OH))₂(IO₃)]₂.

Formula	Mg(H ₂ O) ₆ [(IO ₂ (OH)) ₂ (IO ₃)] ₂
Formula weight	1185.84
Temperature/K	300.0
Crystal system	Monoclinic
Space group	<i>P</i> 2 ₁ / <i>c</i>
<i>a</i> /Å	7.1697(2)
<i>b</i> /Å	21.3401(5)
<i>c</i> /Å	7.6048(2)
$\alpha/^\circ$	90
$\beta/^\circ$	107.1430(10)
$\gamma/^\circ$	90
Volume/Å ³	1111.86(5)
<i>Z</i>	2
ρ_{calc} g/cm ³	3.542
μ/mm^{-1}	8.515
<i>F</i> (000)	1076.0
Crystal size/mm ³	0.24 × 0.193 × 0.16
Radiation	MoKα ($\lambda = 0.71073$)
2θ range for data collection/°	5.922 to 56.614
Index ranges	-9 ≤ <i>h</i> ≤ 9, -28 ≤ <i>k</i> ≤ 28, -10 ≤ <i>l</i> ≤ 10
Reflections collected	27316
Independent reflections	2770 [$R_{\text{int}} = 0.0279$, $R_{\text{sigma}} = 0.0137$]
Data/restraints/parameters	2770/4/148
Goodness-of-fit on <i>F</i> ²	1.166
Final <i>R</i> indexes [$ I \geq 2\sigma(I)$] ^[a]	$R_1 = 0.0149$, $wR_2 = 0.0269$
Final <i>R</i> indexes [all data]	$R_1 = 0.0174$, $wR_2 = 0.0274$
Largest diff. peak/hole / e Å ⁻³	0.57/-0.41

^[a] $R_1 = \sum ||F_o| - |F_c|| / \sum |F_o|$ and $wR_2 = [\sum w(F_o^2 - F_c^2)^2 / \sum wF_o^4]^{1/2}$ for $F_o^2 > 2\sigma(F_o^2)$

Table S2. Atomic coordinates ($\times 10^4$), equivalent isotropic displacement parameters ($\text{\AA}^2 \times 10^3$) and bond valence sum calculations for $\text{Mg}(\text{H}_2\text{O})_6[(\text{IO}_2(\text{OH}))_2(\text{IO}_3)]_2$. U_{eq} is defined as 1/3 of the trace of the orthogonalized U_{ij} tensor.

Atoms	x	y	z	U_{eq}	BVS
Mg1	0	5000	5000	23.2(3)	2.14
I1	5317.4(2)	7932.6(2)	9670.8(2)	15.61(4)	5.12
I2	5679.9(2)	6125.1(2)	9976.8(2)	16.64(4)	5.23
I3	1015.4(2)	6779.8(2)	277.4(2)	17.26(5)	5.22
O1	5428(3)	8823.4(9)	9970(3)	27.4(5)	-1.28
O2	2838(3)	4757.0(10)	6623(3)	30.9(5)	-0.32
O3	9269(3)	7427.0(10)	467(3)	29.2(5)	-1.34
O4	5841(3)	5612.0(9)	8132(3)	23.8(4)	-1.68
O5	9808(3)	6181.8(10)	1157(3)	29.5(5)	-1.83
O6	2716(3)	7873.6(9)	9139(3)	25.0(4)	-1.76
O7	5192(3)	6841.9(9)	8625(3)	24.3(4)	-1.94
O8	877(3)	4999.8(11)	2625(3)	36.2(5)	-0.35
O9	5594(3)	8025.7(9)	7424(3)	23.0(4)	-1.98
O10	649(3)	5929.7(10)	5322(3)	35.7(5)	-0.39
O11	3237(3)	5932.1(9)	9996(3)	27.5(4)	-2.01
O12	9842(3)	6694.1(9)	7861(3)	24.6(4)	-1.77

Table S3. Selected bond lengths (\AA) for $\text{Mg}(\text{H}_2\text{O})_6[(\text{IO}_2(\text{OH}))_2(\text{IO}_3)]_2$.

Atom	Atom	Length/ \AA	Atom	Atom	Length/ \AA
I1	O1	1.9133(19)	I3	O11	2.461(2)
I1	O6	1.7928(19)	I3	O12	1.7909(19)
I1	O7	2.4529(19)	Mg1	O2	2.110(2)
I1	O9	1.7883(18)	Mg1	O2 ¹	2.110(2)
I2	O4	1.8102(18)	Mg1	O8	2.080(2)
I2	O7	1.8187(18)	Mg1	O8 ¹	2.080(2)
I2	O11	1.8037(19)	Mg1	O10	2.036(2)
I3	O3	1.898(2)	Mg1	O10 ¹	2.036(2)
I3	O5	1.7796(19)			

¹-X,1-Y,1-Z

Table S4. Bond Angles for Mg(H₂O)₆[(IO₂(OH))₂(IO₃)]₂.

Atom	Atom	Atom	Angle/°	Atom	Atom	Atom	Angle/°
O1	I1	O7	167.84(7)	O8 ¹	Mg1	O2 ¹	91.25(9)
O6	I1	O1	95.78(9)	O8 ¹	Mg1	O2	88.75(9)
O6	I1	O7	85.64(8)	O8	Mg1	O2 ¹	88.75(9)
O9	I1	O1	89.47(9)	O8	Mg1	O2	91.25(9)
O9	I1	O6	101.13(9)	O8 ¹	Mg1	O8	180.00(13)
O9	I1	O7	78.42(8)	O10	Mg1	O2 ¹	88.72(9)
O4	I2	O7	96.66(9)	O10 ¹	Mg1	O2 ¹	91.28(9)
O11	I2	O4	98.76(9)	O10 ¹	Mg1	O2	88.72(9)
O11	I2	O7	99.87(9)	O10	Mg1	O2	91.28(9)
O3	I3	O11	179.10(8)	O10 ¹	Mg1	O8	90.71(9)
O5	I3	O3	95.07(10)	O10	Mg1	O8	89.29(9)
O5	I3	O11	84.53(8)	O10	Mg1	O8 ¹	90.71(9)
O5	I3	O12	100.32(10)	O10 ¹	Mg1	O8 ¹	89.29(9)
O12	I3	O3	91.80(9)	O10	Mg1	O10 ¹	180.0
O12	I3	O11	87.48(8)	O2	Mg1	O2 ¹	180.0

¹-X,1-Y,1-Z**Table S5.** Hydrogen atom coordinates ($\text{\AA} \times 10^4$) and isotropic displacement parameters ($\text{\AA}^2 \times 10^3$) for Mg(H₂O)₆[(IO₂(OH))₂(IO₃)]₂.

Atom	x	y	z	<i>U</i> _{eq}
H1	5525.72	8925.27	970.54	56(13)
H2A	3381.08	4483.57	6136.72	63(14)
H2B	3532.18	5025.17	6942.32	61(15)
H3	9870.41	7699.62	1166.96	44
H8A	1673.63	4825.69	2299.3	69(15)
H8B	656.73	5291.29	2031.4	67(15)
H10A	969.11	6129.64	4544.23	54
H10B	568.81	6123.34	6216.53	54

Table S6. Hydrogen bonds in $\text{Mg}(\text{H}_2\text{O})_6[(\text{IO}_2(\text{OH}))_2(\text{IO}_3)]_2$.

D-H	$d(\text{D-H})/\text{\AA}$	$d(\text{H}\cdots\text{A})/\text{\AA}$	$\angle \text{D-H}\cdots\text{A}/^\circ$	$d(\text{D}\cdots\text{A})/\text{\AA}$	A
O3-H3	0.820	1.830	147.77	2.561	O12
O10-H10A	0.815	2.465	134.53	3.092	O5
O10-H10A	0.815	2.533	141.52	3.211	O6
O10-H10B	0.812	1.924	164.95	2.717	O12
O1-H1	0.775	1.873	164.32	2.627	O4
O8-H8A	0.781	2.121	170.20	2.894	O4
O8-H8B	0.758	2.046	161.13	2.774	O5
O2-H2A	0.845	1.961	177.67	2.805	O1
O2-H2B	0.750	2.060	167.49	2.797	O4

Table S7. List of reported birefringence compounds in alkali, alkaline earth, and rare earth metal cations-containing iodates/fluoroiodates system.

compound	Δn (@1064 nm)	refs.
KIO ₃	0.1442	¹
KIO ₂ F ₂	0.043	²
RbIO ₃	0.063	³
RbIO ₂ F ₂	0.058	³
NaI ₃ O ₈	0.213*	⁴
CsIO ₃	0.19	⁵
CsIO ₂ F ₂	0.046	⁵
Cs ₃ (IO ₂ F ₂) ₃ ·H ₂ O	0.093	⁵
Cs(IO ₂ F ₂) ₂ ·H ₅ O ₂	0.086	⁵
Ba(IO ₂ F ₂) ₂	0.092	⁶
SrI ₂ O ₅ F ₂	0.18	⁶
Sr(IO ₃) ₂	0.093	⁶
K ₂ Na(IO ₃) ₂ (I ₃ O ₈)	0.055	⁷
α -LiIO ₃	0.1399 (@ 1100 nm)	⁸
α -HIO ₃	0.1372 (@ 1100 nm)	⁸
NH ₄ IO ₃	0.082 (@589 nm)	⁹
YI ₅ O ₁₄	0.091	¹⁰
GdI ₅ O ₁₄	0.092	¹⁰
Ce(IO ₃) ₄	0.039	¹¹
Mg(H ₂ O) ₆ [(IO ₂ (OH)) ₂ (IO ₃)] ₂	0.230	this work

* Calculate this time.

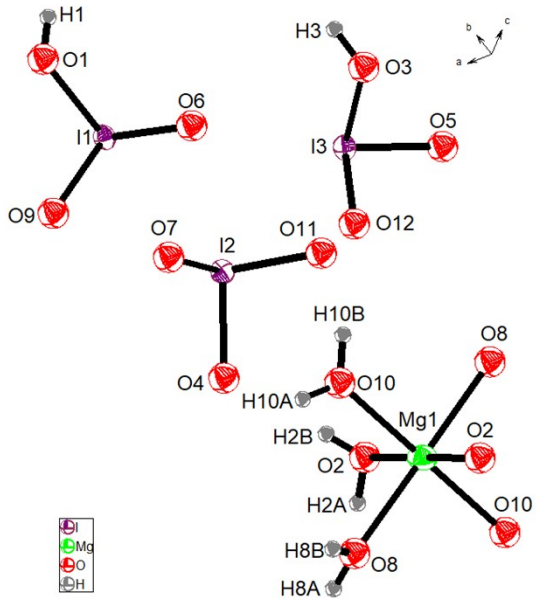


Fig. S1. Asymmetric unit of $\text{Mg}(\text{H}_2\text{O})_6[(\text{IO}_2(\text{OH}))_2(\text{LO}_3)]_2$. The ellipsoids are drawn at 50% probability level.

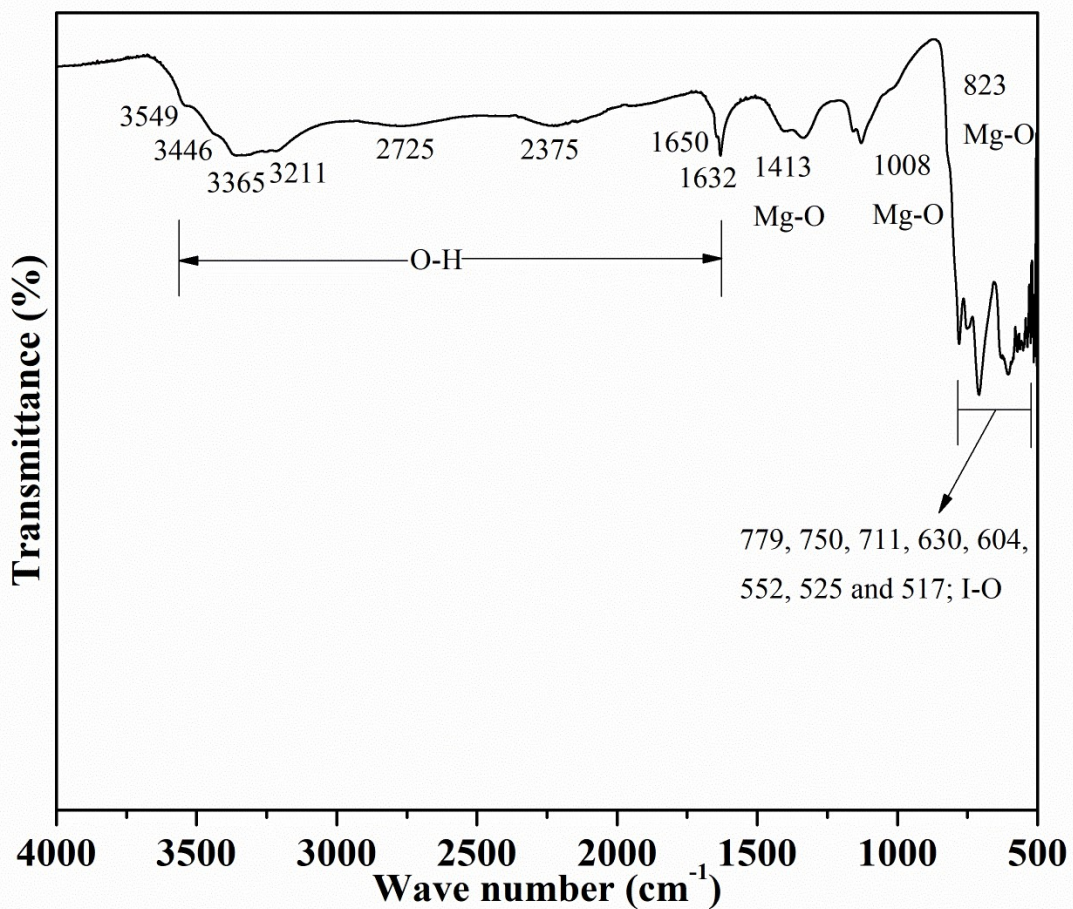


Fig. S2. IR spectrum of $\text{Mg}(\text{H}_2\text{O})_6[(\text{IO}_2(\text{OH}))_2(\text{LO}_3)]_2$.

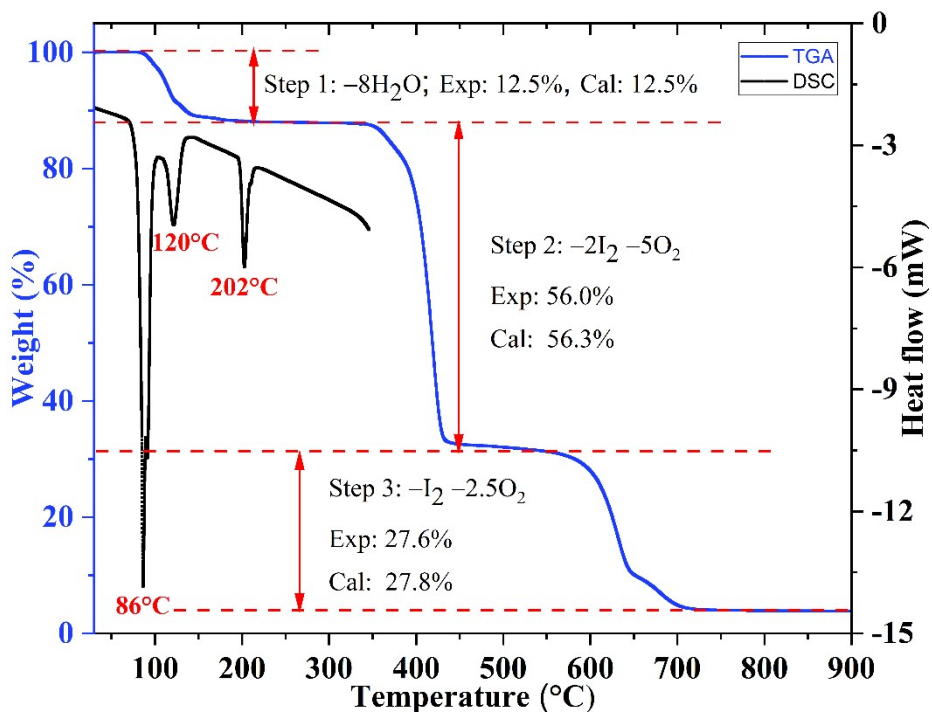
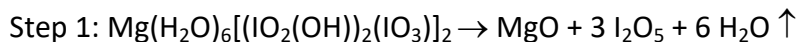
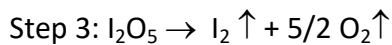
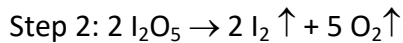


Fig. S3. TGA and DSC diagrams of $\text{Mg}(\text{H}_2\text{O})_6[(\text{IO}_2(\text{OH}))_2(\text{IO}_3)]_2$.

In $\text{Mg}(\text{H}_2\text{O})_6[(\text{IO}_2(\text{OH}))_2(\text{IO}_3)]_2$, six H_2O , four $\text{IO}_2(\text{OH})$, and two IO_3 groups exist. The H_2O and OH units from the $\text{IO}_2(\text{OH})$ group are easily released in step 1 as observed from other similar reported compounds.¹² The observation is in agreement with the endothermic peaks at 86 to 204 °C in the DSC diagram.



In steps 2 and 3, the rest of I_2O_5 group was decomposed. It also could be found in many other iodates, such as $\text{HBa}_{2.5}(\text{IO}_3)_6(\text{I}_2\text{O}_5)$ and $\text{HBa}(\text{IO}_3)(\text{I}_4\text{O}_{11})$.¹³



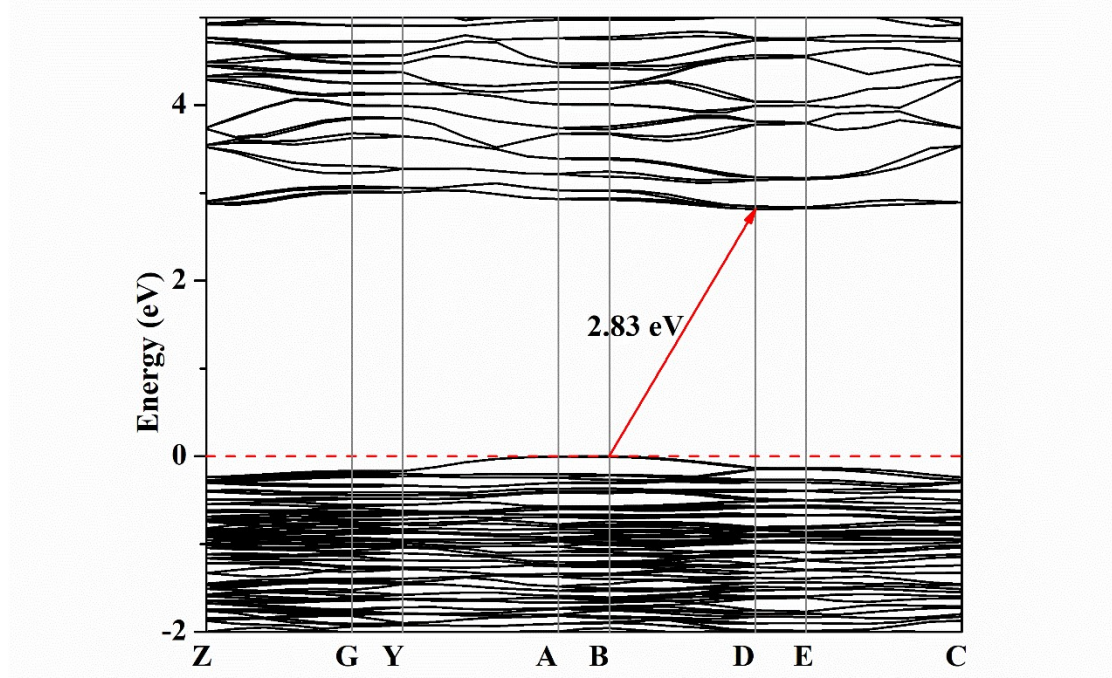


Fig. S4. Band structure for $\text{Mg}(\text{H}_2\text{O})_6[(\text{IO}_2(\text{OH}))_2(\text{LO}_3)]_2$.

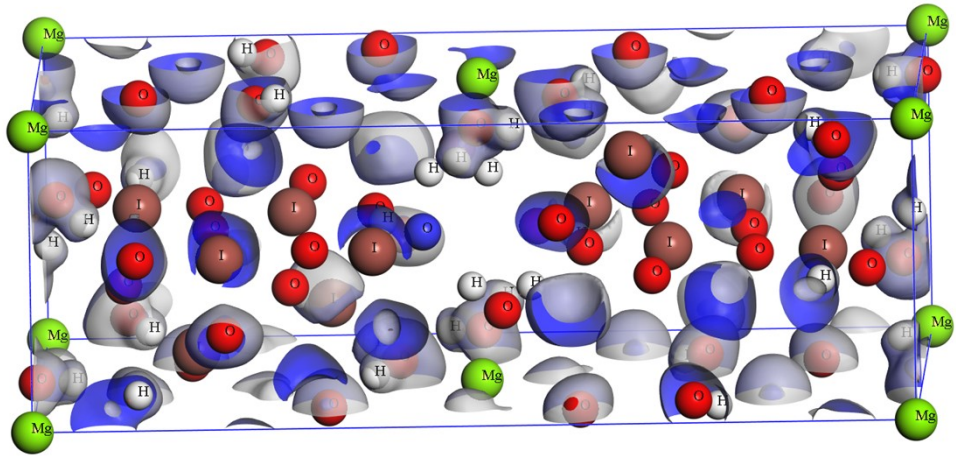


Fig. S5. The electron density difference map of $\text{Mg}(\text{H}_2\text{O})_6[(\text{IO}_2(\text{OH}))_2(\text{IO}_3)]_2$.

References

1. X. Yin, M. K. Lü , S. J. Zh and F. Q. Li, Nonlinear optical properties of perfectly polarized KIO_3 single crystal, *Chinese Phys. Lett.*, 1992, **9**, 77–78.
2. J. G. Bergman and G. R. Crane, Structural aspects of nonlinear optics: Optical properties of KIO_2F_2 and its related iodates, *J. Chem. Phys.*, 1974, **60**, 2470–2474.
3. Q. Wu, H. M. Liu, F. C. Jiang, L. Kang, L. Yang, Z. S. Lin, Z. G. Hu, X. G. Chen, X. G. Meng and J. G. Qin, RbIO_3 and RbIO_2F_2 : Two Promising Nonlinear Optical Materials in Mid-IR Region and Influence of Partially Replacing Oxygen with Fluorine for Improving Laser Damage Threshold, *Chem. Mater.*, 2016, **28**, 1413–1418.
4. D. Phanon and I. Gautier-Luneau, Promising Material for Infrared Nonlinear Optics: NaI_3O_8 Salt Containing an Octaoxotriiodate(V) Anion Formed from Condensation of $[\text{IO}_3]^-$ Ions, *Angew. Chem. Int. Ed.*, 2007, **46**, 8488–8491.
5. M. Zhang, C. Hu, T. Abudouwufu, Z.H. Yang and S.L. Pan, Functional Materials Design via Structural Regulation Originated from Ions Introduction: A Study Case in Cesium Iodate System, *Chem. Mater.*, 2018, **30**, 1136–1145.
6. M.Q. Gai, T.H. Tong, Y. Wang, Z.H. Yang and S.L. Pan, New Alkaline-Earth Metal Fluoroiodates Exhibiting Large Birefringence and Short Ultraviolet Cutoff Edge with Highly Polarizable $(\text{IO}_3\text{F})^2-$ Units, *Chem. Mater.*, 2020, **32**, 5723–5728.
7. T. Abudouwufu, M. Zhang, S.C. Cheng, H. Zeng, Z.H. Yang and S.L. Pan, $\text{K}_2\text{Na}(\text{IO}_3)_2(\text{I}_3\text{O}_8)$ with Strong Second Harmonic Generation Response Activated by Two Types of Isolated Iodate Anions, *Chem. Mater.*, 2020, **32**, 3608–3614.
8. V. G. Dmitriev, G. G. Gurzadyan, D. N. Nikogosyan, Handbook of nonlinear optical crystals, Springer, 2013.
9. E. T. Keve, S. C. Abrahams and J. L. Bernstein, Pyroelectric Ammonium Iodate, a Potential Ferroelastic: Crystal Structure, *J. Chem. Phys.*, 1971, **54**, 2556–2563.
10. J. Chen, C. L. Hu, F. F. Mao, B. P. Yang, X. H. Zhang and J. G. Mao, $\text{REI}_5\text{O}_{14}$ ($\text{RE}=\text{Y}$ and Gd): Promising SHG Materials Featuring the Semicircle-Shaped $\text{I}_5\text{O}_{14}^{3-}$ Polyiodate Anion, *Angew. Chem. Int. Ed.*, 2019, **58**, 11666–11669.
11. T. H. Wu, X. X. Jiang, C. Wu, H. Y. Sha, Z. J. Wang, Z. S. Lin, Z. P. Huang, X. F. Long, M. G. Humphrey and C. Zhang, From $\text{Ce}(\text{IO}_3)_4$ to $\text{CeF}_2(\text{IO}_3)_2$: fluorinated homovalent substitution simultaneously enhances SHG response and bandgap for mid-infrared nonlinear optics, *J. Mater. Chem. C*, 2021, **9**, 8987–8993.
12. X. Xu, B. P. Yang, C. Huang and J. G. Mao, Explorations of New Second-Order Nonlinear Optical Materials in the Ternary Rubidium Iodate System: Noncentrosymmetric β - $\text{RbIO}_3(\text{HIO}_3)_2$ and Centrosymmetric $\text{Rb}_3(\text{IO}_3)_3(\text{I}_2\text{O}_5)(\text{HIO}_3)_4(\text{H}_2\text{O})$, *Inorg. Chem.*, 2014, **53**, 1756–1763.
13. F. F. Mao, C. L. Hu, J. Chen, B. L. Wu and J. G. Mao, $\text{HBa}_{2.5}(\text{IO}_3)_6(\text{I}_2\text{O}_5)$ and $\text{HBa}(\text{IO}_3)(\text{I}_4\text{O}_{11})$: Explorations of Second-Order Nonlinear Optical Materials in the Alkali-Earth Polyiodate System, *Inorg. Chem.*, 2019, **58**, 3982–3989.